

Light Trajectories and Thermal Shadows casted by Black Holes in a Cavity

A. Belhaj ^{1*}, H. Belmahi ^{1†}, M. Benali ^{1‡}, M. Oualaid^{1§}, M. B. Sedra^{2¶}

¹ Département de Physique, Equipe des Sciences de la matière et du rayonnement, ESMaR

Faculté des Sciences, Université Mohammed V de Rabat, Rabat, Morocco

² Material and subatomic physics laboratory, LPMS, University of Ibn Tofail, Kenitra, Morocco

June 2, 2022

Abstract

We explore the shadows and the photon rings casted by black holes in cavity. Placing the observer inside such an isothermal background, we examine the influence of the cavity temperature T_{cav} and the charge Q on the involved optical aspect. After studying the effect of the horizon radius by varying Q , we investigate the thermal behaviors of the black hole shadows in a cavity. For fixed charge values, we find that the shadow radius r_s increases by decreasing T_{cav} . Varying such a temperature, we discuss the associated energy emission rate. After that, we show that the curves in the $r_s - T_{cav}$ plane share similarities with the $G - T$ curves of the Anti de Sitter (AdS) black holes. Then, we study the trajectory of the light rays casted by black holes in a cavity. We further observe that the light trajectory behaviors are different than the ones of the non rotating black holes due to the cavity effect. Finally, we provide evidence for the existence of an universal ratio defined in terms of the photon sphere radius and the impact parameter. Concretely, we obtain a optical ratio $\frac{b_{sp}}{r_{sp}} \sim \sqrt{3}$.

Keywords: Black holes in cavity, Thermodynamics, Shadow formalism, energy emission rate, Hawking-Page phase transition, Light trajectories.

*a-belhaj@um5r.ac.ma

†hajar_belmahi@um5.ac.ma

‡mohamed_benali4@um5.ac.ma

§mohamed_oualaid@um5.ac.ma

¶mysedra@yahoo.fr

|| Authors in alphabetical order.

Contents

1	Introduction	3
2	Black holes in a cavity	4
3	Shadow behaviors of the black holes in a cavity system	5
4	Shadow thermal behaviors of black holes	9
5	Trajectories of the light rays by black holes in a cavity	12
6	Conclusion and open questions	15

1 Introduction

Recently, the study of the optical and the thermodynamics of the black hole has brought many interesting results associated with classical and quantum gravity models. These findings have been supported by detections and observational investigations of such fascinating objects. Concretely, the Event Horizon Telescope (EHT) international collaboration has provided an image of an accretion flow through the vicinity of the supermassive black hole in M87* [1–3]. In this image, a dark interior has been observed. This region called shadow is surrounded by a bright ring known as the photon sphere. Since the elaboration of such an image and the associated data by EHT, various works dealing with the geometric properties of the black hole shadows have been proposed by examining the involved sizes and shapes [4–19]. In four dimensions, it has been shown that the non-rotating black hole solutions exhibit a perfect circular geometry where the size can be controlled by certain parameters as the charge [7, 20, 21]. For the rotating black holes, however, the circular configuration is deformed and distorted generating non trivial shapes including D and cardioid ones [22–25]. It has been remarked that EHT data can be exploited to impose constraints on certain black hole parameters. These constraints could be used to build models matching with the EHT observations considered as a reference for testing the obtained theoretical results.

Beside the optical aspect, the black hole thermodynamics has received also a remarkable interest showing non trivial results corresponding to the criticality and the stability behaviors. A crucial focus has been devoted to the study of the black holes on the AdS geometries [26–29]. The needed quantities have been nicely computed for various gravity theories. Considering the cosmological as a pressure, certain black holes show similarities with van der Waals fluid systems where some universalities have been obtained. It has been revealed that the AdS black holes can be in a stable thermal equilibrium with radiations [26, 28, 30, 31]. Hawking and Page (HP) have provided theoretical evidence for the existence of certain transitions in the phase space of the (non-rotating uncharged) Schwarzschild-AdS black hole. A first order phase transition in the charged (non-rotating) Reissner Nordstrom-AdS (RN-AdS) black hole space-time has been studied in different backgrounds including Dark Energy (DE) and Dark Matter (DM) [20, 32, 33]. The effect of such a dark sector on the optical aspect has been also investigated for different backgrounds. In this way, the shadows and the deflection angle of the light rays by black holes in arbitrary dimensions have been discussed in [12, 20–22]. The effect of DE and the space-time dimension on the involved optical quantities has been inspected. In [23, 25], for instance, the influence of DM on the shadows and the photon rings of a stringy black hole illuminated by certain accretions has been also studied.

Motivated by the investigations on singular space-times, interplays between the black hole thermodynamics and the optical properties have been established. It has been shown that the shadow size can provide information on the HP phase transitions, the critical behaviors and the microstructure states of the black holes living in AdS geometries [34–36]. It can reflect also data on the geothermodynamics by providing certain universalities [37]. It has been shown that the relation between the shadow and the thermodynamics of the black hole has

been also developed for regular space-times [38]. Using the elliptic function analysis, it has been explored further a fundamental connection between the AdS black hole thermodynamics and the deflection angle of the light rays. Concretely, various thermodynamics behaviors of such black holes have been approached in terms the deflection angle variations [39].

More recently, it has been shown that the black holes on the AdS geometries share similarities with certain black holes enclosed by an isothermal cavity. The latter has been considered as a tool to provide a stable solution [40–44]. Precisely, it has been revealed that the Schwarzschild black holes in a cavity can be thermally stable. They involve the phase structures and transition behaviors similar to the ones appearing in the Schwarzschild-AdS black holes. A similar interplay has been observed in the Reissner- Nordstrom (RN) black holes, by considering canonical ensembles. The phase structures of certain extended models in a cavity have been investigated where the Hawking-Page-like and van der Waals-like phase transitions have taken place [45].

The aim of this work is to explore for the first time the optical behaviors of the black holes in a cavity. Precisely, we investigate the shadows and the photon rings casted by black holes surrounded by such an isothermal generic space, by examining the effect of the cavity temperature T_{cav} and the charge Q . After studying the effect of the horizon radius on the visualizing shadows of the proposed black holes by varying the charge, we move to study thermal behaviors of the involved shadows. For fixed charge values, we observe that the shadow radius r_s increases by decreasing the cavity temperature T_{cav} . Varying such a temperature, we discuss the energy emission rate. Moreover, we show that the curves in the $r_s - T_{cav}$ plane share similarities with the $G - T$ curves of the AdS black holes. Then, we investigate the trajectory of the light rays casted by the black holes in a cavity. We reveal that the light trajectories are different than the light ray behaviors of the non rotating black holes due to the cavity effect. Finally, we provide evidence for the existence of an universal ratio associated with the photon sphere radius and the impact parameter. Precisely, we find the optical ratio $\frac{b_{sp}}{r_{sp}} \sim \sqrt{3}$.

This paper is organized as follows. In section 2, we present a concise review on the black holes surrounded by a cavity. In section 3, we approach the black hole shadows in terms of the horizon radius. Section 4 is devoted to the thermal behaviors of such shadows. In section 5, we discuss the trajectories of the light rays casted by the black holes in a cavity. Finally, section 6 ends up with certain conclusions and open questions.

2 Black holes in a cavity

In this section, we present a concise review on the black holes in a cavity background. In particular, we give the associated relevant concepts. It is recalled that in asymptotically AdS geometries, the black holes can be considered thermodynamically stable [40, 45]. In this way, the AdS boundary serves as a reflective wall. Alternatively, various works have reported that the black holes enclosed by a cavity can be also thermally stable. It has been suggested that

the cavity presence could overcome the thermodynamics stability problem of the black holes in asymptotically flat spaces. These activities push one to inspect other aspects including the optical ones. This could unveil certain interesting behaviors by considering static and spheric metric structures of the black holes in a cavity physical system. In this way, the 4-dimensional metric solution can be expressed as follows

$$ds^2 = -f(r)dt^2 + \frac{dr^2}{f(r)} + r^2(d\theta^2 + \sin^2\theta d\phi^2), \quad (2.1)$$

where $f(r)$ is the function metric of a black hole in a cavity. In terms of the involved parameters [45], this metric function takes the following form

$$f(r) = \left(1 - \frac{r_+}{r}\right)\left(1 - \frac{Q^2}{r r_+}\right). \quad (2.2)$$

In this relation, r_+ indicates the horizon radius given by

$$r_+ = m + \sqrt{m^2 - Q^2}, \quad (2.3)$$

where m and Q are the charge and the mass parameters of the black holes, respectively. For $Q = 0$, however, we recover the Schwarzschild solution [46]. A close examination shows that many models could be approached depending on the observer positions. For simplicity reasons, however, we could place the observer inside the cavity surrounded region. This situation can be ensured by the following constraint

$$\begin{cases} r_{cav} > r_+ & (2.4) \\ r_{cav} > r_{ob}, & (2.5) \end{cases}$$

being interpreted as thermodynamic and optical conditions, respectively. In Fig.(1), we illustrate the representation of a black hole in a cavity with the above requirements.

The red line represents the light transmitting to the observer placed at r_{ob} being smaller to the cavity radius r_{cav} . However, the blue surface corresponds to the equatorial plane.

3 Shadow behaviors of the black holes in a cavity system

In this section, we investigate the optical properties of the black hole in a cavity. In particular, we study the shadow behaviors by varying the involved black hole parameters. Precisely, we approach the shadow geometrical configurations in terms of the one-dimensional real closed curves obtained from the equation of motion [7, 21, 24]. The geometric behaviors of such curves are controlled by r_+ and Q parameters. To start, we consider the Hamilton-Jacobi equation

$$\frac{\partial S}{\partial \tau} = -\frac{1}{2}g^{\alpha\beta}p_\alpha p_\beta, \quad (3.1)$$

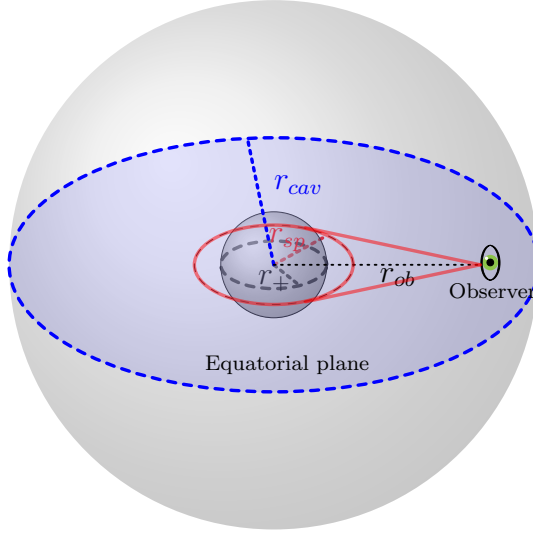


Figure 1: Illustrating black hole in a cavity.

where S and λ are the Jacobi action and the affine parameter along the geodesics, respectively. p^α represents the conjugate momentum of the black hole in a cavity system. In the spherically symmetric spacetime, the Hamiltonian which describes the photon motion can be expressed as follows

$$H = \frac{1}{2} g^{\alpha\beta} p_\alpha p_\beta = 0. \quad (3.2)$$

Considering a particular motion of the photons in the equatorial plane $\theta = \frac{\pi}{2}$, the Hamiltonian equation reduces to the following form

$$(rf(r)p_r)^2 - r^2 p_t^2 + f(r)p_\phi^2 = 0. \quad (3.3)$$

Apply the Hamiltonian-Jacobi formalism, the equations describing the motion of the photons can be formulated as

$$\begin{aligned} \frac{dt}{d\lambda} &= \frac{E}{f(r)} \\ \frac{dr}{d\lambda} &= \pm \sqrt{f(r) \left(\frac{E^2}{f(r)} - \frac{L^2}{r^2} \right)} \\ \frac{d\phi}{d\lambda} &= -\frac{L}{r^2} \end{aligned} \quad (3.4)$$

where $E = -p_t$ and $L = p_\phi$ are the conserved total energy and the conserved angular momentum of the photon, respectively. It turns out that the geometric shape of a black hole can be completely described by the limit of their shadows being the visible shape of the unstable closed geodesic curves of the photons. To approach such behaviors, one can exploit the radial equation of motion given by

$$\left(\frac{dr}{d\tau} \right)^2 + V_{eff}(r) = 0, \quad (3.5)$$

where $V_{eff}(r)$ indicates the effective potential for a radial particle motion in the space-time. In particular, it reads as

$$V_{eff} = f(r) \left(\frac{L^2}{r^2} - \frac{E^2}{f(r)} \right). \quad (3.6)$$

An examination reveals that the maximal value of the effective potential corresponds to the radius of the circular orbits r_{sp} . To get the radius of photon unstable circles, one should consider the following constraint

$$V_{eff} = \frac{dV_{eff}}{dr} \Big|_{r=r_{sp}} = 0. \quad (3.7)$$

Using Eq.(3.6) and Eq.(3.7), one can obtain

$$V_{eff}|_{r=r_{sp}} = \frac{dV_{eff}}{dr} \Big|_{r=r_{sp}} = \begin{cases} f(r_{sp}) \left(\frac{L^2}{r_{sp}^2} - \frac{E^2}{f(r_{sp})} \right) = 0, \\ L^2 \left(\frac{r_{sp}f'(r_{sp}) - 2f(r_{sp})}{r_{sp}^3} \right) = 0, \end{cases} \quad (3.8)$$

where the notation $f'(r) = \frac{\partial f(r)}{\partial r}$ has been considered. By the help of the Eq.(3.8), we can obtain the equation constraint concerning the radius of the unstable photons sphere via the relation

$$r_{sp}f'(r_{sp}) - 2f(r_{sp}) = 0. \quad (3.9)$$

The real and the positive solution of this equation is given by

$$r_{sp} = \frac{3(Q^2 + r_+^2) + \sqrt{9Q^4 - 14Q^2r_+^2 + 9r_+^4}}{4r_+}. \quad (3.10)$$

It has been remarked that the photon sphere radius r_{sp} which depends on the charge Q and the horizon radius r_+ can recover certain previous results. Taking $Q = 0$ and $r_+ = 2M$, we obtain the radius of the unstable photon sphere of the Schwarzschild black hole solution [7, 9, 21]. By the help of the radial and the angular geodesic equations, the orbit equation for the photon reads as

$$\frac{dr}{d\phi} = \pm \frac{r^2}{L} \sqrt{f(r) \left(\frac{E^2}{f(r)} - \frac{L^2}{r^2} \right)}. \quad (3.11)$$

The photon orbit is constrained by

$$\frac{dr}{d\phi} \Big|_{r=r_{sp}} = 0. \quad (3.12)$$

Using the Eq.(3.12), the previous equation take the following form

$$\frac{dr}{d\phi} = \pm r \sqrt{f(r) \left[\frac{r^2 f(r_{sp})}{r_{sp}^2 f(r)} - 1 \right]}. \quad (3.13)$$

Considering the light ray sent from a static observer situated at r_{ob} inside the cavity and transmitted into the past with an angle α_{ob} , we have

$$\cot \alpha_{ob} = \frac{\sqrt{g_{rr}}}{\sqrt{g_{\phi\phi}}} \frac{dr}{d\phi} \Big|_{r=r_{ob}} = \frac{1}{r \sqrt{f(r)}} \frac{dr}{d\phi} \Big|_{r=r_{ob}}. \quad (3.14)$$

Exploiting Eq.(3.14), one obtain the angle of the observer as a function of the various parameters

$$\sin^2 \alpha_{ob} = \frac{f(r_{ob})r_{sp}^2}{r_{ob}^2 f(r_{sp})}. \quad (3.15)$$

In this context, one can get the angular radius of the black hole shadows as a function of the circular orbit radius of the photon appearing in Eq.(3.10). Precisely, the shadow radius of the black hole observed by a static observer placed at r_{ob} is given by

$$r_s = r_{ob} \sin \alpha_{ob} = R \sqrt{\frac{f(r_{ob})}{f(R)}} \Big|_{R=r_{sp}}. \quad (3.16)$$

According to [47], the apparent shape of the black hole shadow in a cavity system can be obtained by using the celestial coordinates x and y which can be expressed as

$$\begin{aligned} x &= \lim_{r_0 \rightarrow \infty} \left(-r_0^2 \sin \theta_0 \frac{d\phi}{dr} \Big|_{(r_0, \theta_0)} \right), \\ y &= \lim_{r_0 \rightarrow \infty} \left(r_0^2 \frac{d\theta}{dr} \Big|_{(r_0, \theta_0)} \right). \end{aligned} \quad (3.17)$$

In Fig(2), we plot the shadow geometry for different values of the charge Q . As expected, the

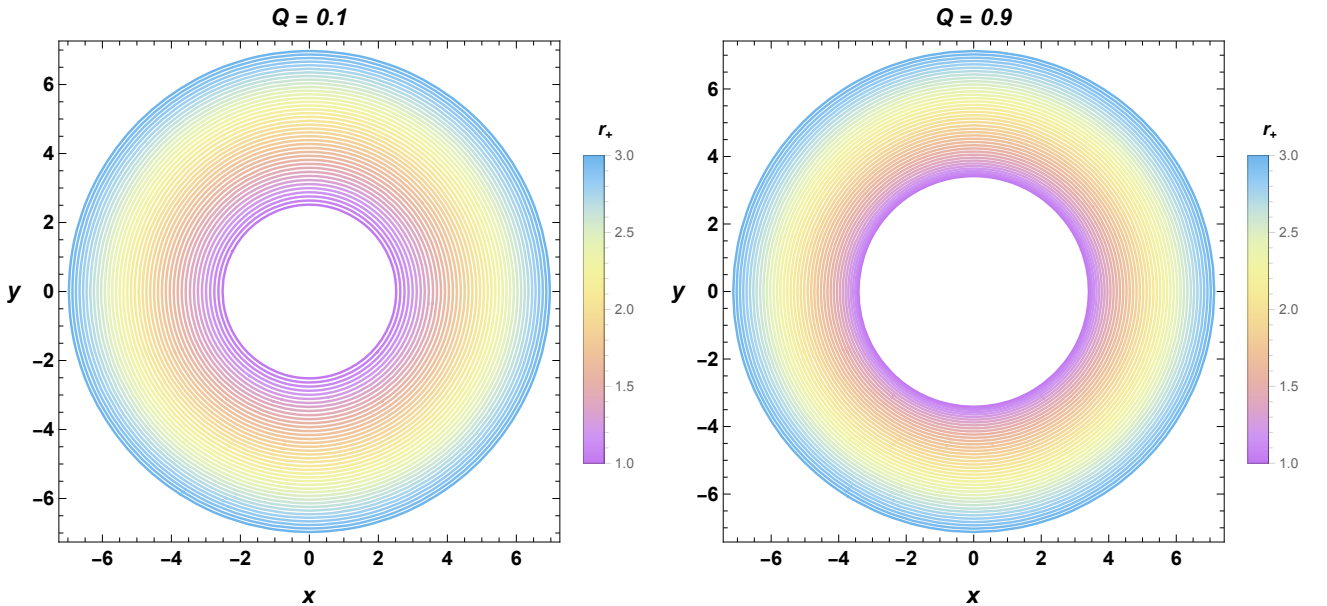


Figure 2: *Shadow variations of a black hole in a cavity system as a function of r_+ for fixed values of Q by placing the observer in the equatorial plane and taking $r_{ob} = 15$ and $r_{cav} = 20$.*

geometry of the shadows is a perfect circular due to the absence of the rotating parameter. It has been remarked that the charge of the black hole in a cavity is a relevant parameter controlling the optical behaviors including the shadow size. Indeed, the latter increases with

the horizon radius. Taking a fixed value of r_+ , the shadow size increases by increasing the charge Q . It is denoted that for $Q = 0$, we recover the shadow of the Schwarzschild black hole [7, 9, 21]. To inspect the shadow radius variation, we consider its variation in terms of r_+ for different values of the charge. This is illustrated in Fig(3). This figure confirms

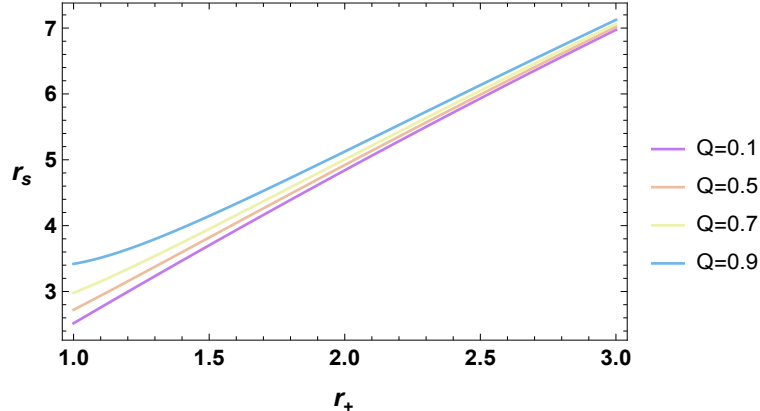


Figure 3: Shadow radius as a function of r_+ for fixed values of the charge. The observer in the equatorial plane and positioned in $r_{ob} = 15$, we take the cavity radius $r_{cav} = 20$.

the previous findings where the radius augments with the charge. This quantity has been interpreted as a geometric parameter controlling the shadow size.

4 Shadow thermal behaviors of black holes

Motivated by certain results associated with the link between the black holes in a cavity and the thermodynamics of the AdS black holes, we study shadow behaviors by varying the cavity temperature. It is recalled that the temperature is a crucial needed quantity to approach the stability behaviors. Indeed, the Hawking temperature is given by

$$T_H = \frac{1}{4\pi} \left. \frac{df(r)}{dr} \right|_{r=r_+}. \quad (4.1)$$

In the cavity system, however, the temperature related to the cavity radius r_{cav} . Concretely, it is expressed as follows

$$T_{cav} = \frac{T_H}{\sqrt{f(r_{cav})}} \quad (4.2)$$

which can be given in terms of the involved physical parameters [40, 41, 45]. According to such works, the calculations provide

$$T_{cav} = \frac{r_+^2 - Q^2}{4\pi r_+ \sqrt{f(r_{cav})}}. \quad (4.3)$$

It has been remarked that the cavity temperature T_{cav} and the shadow geometry in a cavity are controlled by the radius horizon. Inspired by such a link, we investigate the shadow

behaviors by varying the temperature. It has been observed that, for $r_{cav} > r_+$, the temperature of the cavity system is similar to the one of the charged AdS black hole. The only difference is for $r_{cav} = r_+$ where the cavity temperature T_{cav} diverges [45]. As proposed in Fig.(1), the observer is placed inside the cavity to visualize the transmitting lights in terms of the shadow real closed curves. By the help of the method reported in [47], we study the thermal shadow behaviors. In Fig.(4), we illustrate the shadows as functions of the cavity temperature T_{cav} for fixed values of the charge Q . To get a concrete model, we consider a situation where one has $r_{cav} = 20$ and $r_{ob} = 15$. In this way, the shadow size increases by

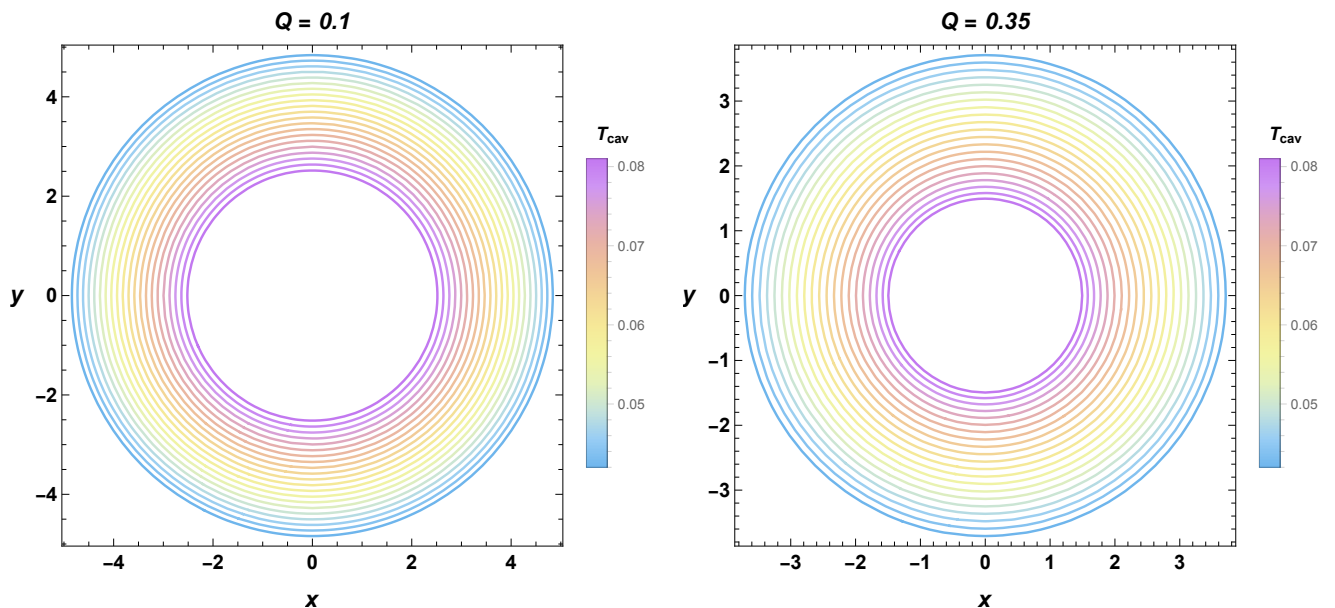


Figure 4: *Shadow behaviors of a black hole in a cavity system as a function of the cavity temperature for fixed values of Q by placing the observer in the equatorial plane and taking $r_{ob} = 15$ and $r_{cav} = 20$.*

decreasing the temperature of the cavity system. It follows from this figure that the charge Q decreases the shadow radius of the black hole in a cavity. Augmenting the charge Q , we observe that the temperature variation is contrary to the horizon radius one as illustrated in Fig.(3). These inverse behaviors come from the relationship between the cavity temperature and the horizon radius r_+ . Indeed, when T_{cav} decreases (increases), r_+ increases (decreases). Moreover, certain properties of the AdS black hole solutions associated with the shadow radius aspect have been conserved in the black hole inside the cavity. In fact, it is an increasing (decreasing) function of the mass (temperature) [9, 21]. Such thermal behaviors push one to inspect other black hole properties needed to support the present findings. The corresponding energy emission rate could be investigated. It is worth noting that near the horizon of the black hole, the quantum fluctuations can create and annihilate pairs of particles. In this way, the particles with positive energies can escape through tunneling from the black hole associated with the Hawking radiation. In what follows, we discuss the involved energy

emission rate in a cavity background. For a distant observer with the above optical and the thermodynamical conditions, the high energy absorption cross section could provide data on the black hole shadows. In this regard, it has been remarked that the absorption cross section of the black hole can oscillate to an approximated constant value $\sigma_{lim} = \pi r_s^2$. The energy emission rate can be written as

$$\frac{d^2 E(\omega)}{d\omega dt} = \frac{2\pi^3 r_s^2 \omega^3}{e^{\frac{\omega}{T_H}} - 1}, \quad (4.4)$$

where ω indicates the emission frequency [21, 23, 24, 48], and where T_H is the associated Hawking temperature. Using the link with the cavity temperature, this expression takes the following form

$$\frac{d^2 E(\omega)}{d\omega dt} = \frac{2\pi^3 r_s^2 \omega^3}{e^{\sqrt{f(r_{cav})} \cdot T_{cav}} - 1}. \quad (4.5)$$

The energy emission rate is illustrated in Fig.(5) as a function of ω by varying T_{cav} and Q . For small values of the cavity temperature, it has been observed that the charge does

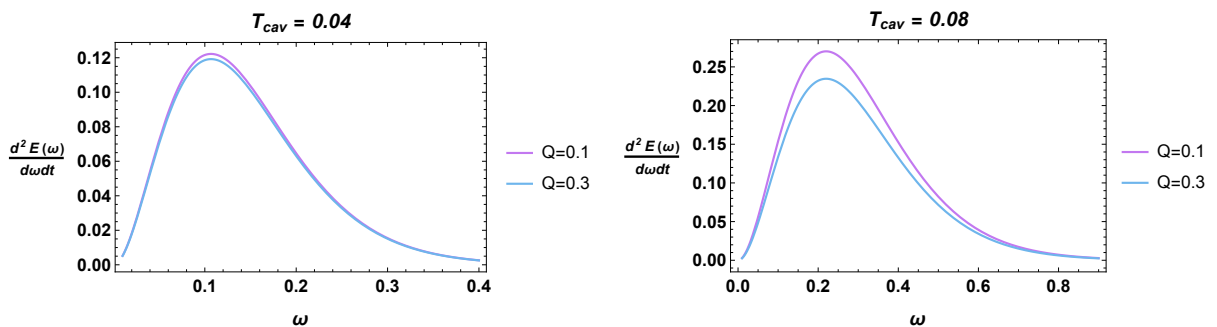


Figure 5: Energy emission rate for different values of T_{cav} and Q , by placing the observer in the equatorial plane and taking $r_{ob} = 15$ and $r_{cav} = 20$.

not bring any relevant effect. Augmenting such a temperature, the energy emission rate maximum increases by decreasing the charge Q . Fixing the charge values, this maximum increases with T_{cav} . This shows that T_{cav} and Q involve opposite effects on the involved optical behaviors to ensure the stability. This finding confirms the previous obtained results dealing with black holes in cavities.

Inspired by the similarities between the black hole thermodynamics in AdS geometries and in isothermal backgrounds, we approach the cavity temperature from an optical point of view. Indeed, we plot in Fig.(6) the cavity temperature as a function of the shadow radius by varying the charge Q . The shadow radius increases by decreasing T_{cav} and decreases with the charge Q . This behavior is confirmed in Fig.(6), by using the optical and the thermodynamical conditions given by the equations Eq.(2.4) and Eq.(2.5) for $r_{ob} = 3$ associated with an observer placed closed to the sphere photon radius of the black hole in a cavity. An examination shows that the curves in the $r_s - T_{cav}$ plane share similarities with the $G - T$ curves of the charged and the rotating AdS black holes, where G and T are the Gibbs free

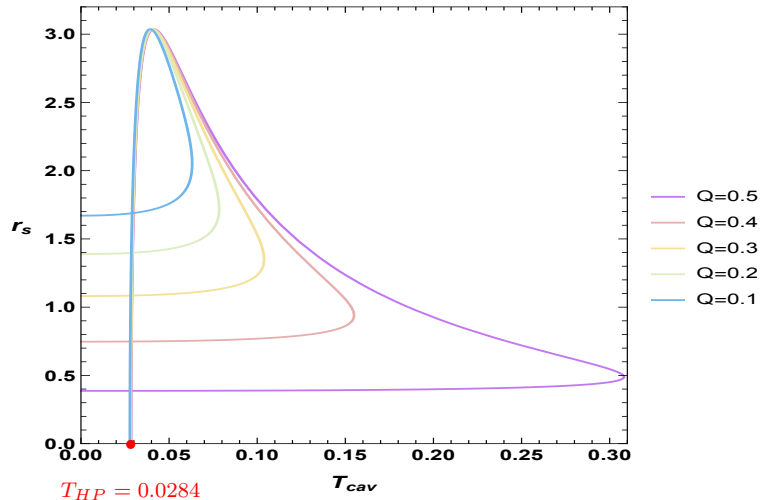


Figure 6: *The behaviors of the shadow radius in terms of the cavity temperature. In particular, we take the observer in the equatorial plane and positioned in $r_{ob} = 3$ and the cavity radius $r_{cav} = 20$.*

energy and the temperature, respectively. To unveil such similar behaviors, we should exploit such thermodynamical quantities. According to [45], the Gibbs free energy expression of a black hole in a cavity takes the following form

$$G = r_{cav} \left[\frac{7 \frac{r_+}{r_{cav}} + \frac{Q^2}{r_+ r_{cav}} - 8}{12 \sqrt{f(r_{cav})}} + \frac{2}{3} \right]. \quad (4.6)$$

Solving the equation $G = 0$, we can get the value of the phase transition temperature T_{HP} . Varying the charge Q parameter, this temperature is found to be constant

$$T_{HP} = 0.0284. \quad (4.7)$$

Moreover, it has been observed that the $r_s - T_{cav}$ curves involve the swallowtail behavior observed in the $G - T$ plane. Indeed, the T_{HP} temperature in the $G - T$ plane coincides with the T_{HP} temperature in the $r_s - T_{cav}$ plane. This result could be used to confirm the relation between the thermodynamics and the optical aspects of the black holes in a cavity. As expected, certain thermal quantities of the black holes including the phase transition temperature T_{HP} can be approached using the shadow findings.

5 Trajectories of the light rays by black holes in a cavity

In this section, we study the trajectory of the light rays casted by the black holes in a cavity. In particular, we determine the light trajectory around the black hole in a cavity by varying the cavity temperature T_{cav} . The light trajectory casted by the black holes in cavities can

be established by using numerical computations associated with the following orbit equation

$$\frac{du}{d\phi} = \sqrt{\frac{1}{b^2} - u^2(1 - ur_+)(1 - \frac{Q^2u}{r_+})}, \quad (5.1)$$

where one has used the change variable $u = \frac{1}{r}$ and where b is the so-called the impact parameter given by $b = \frac{|L|}{E}$ [49, 50]. Using Eq(5.1), we can solve ϕ with respect to u in order to depict the trajectory of the light ray in a cavity background. To approach the trajectory of the light rays casted by the black holes in a such system, we need to find the regions corresponding to the light ray trajectory possibilities. Indeed, they can be determined by the help of the effective potential given by Eq.(3.6). In Fig.(7), we plot such an effective potential as a function of the radial coordinate r for different values of the cavity temperature T_{cav} and the charge Q .

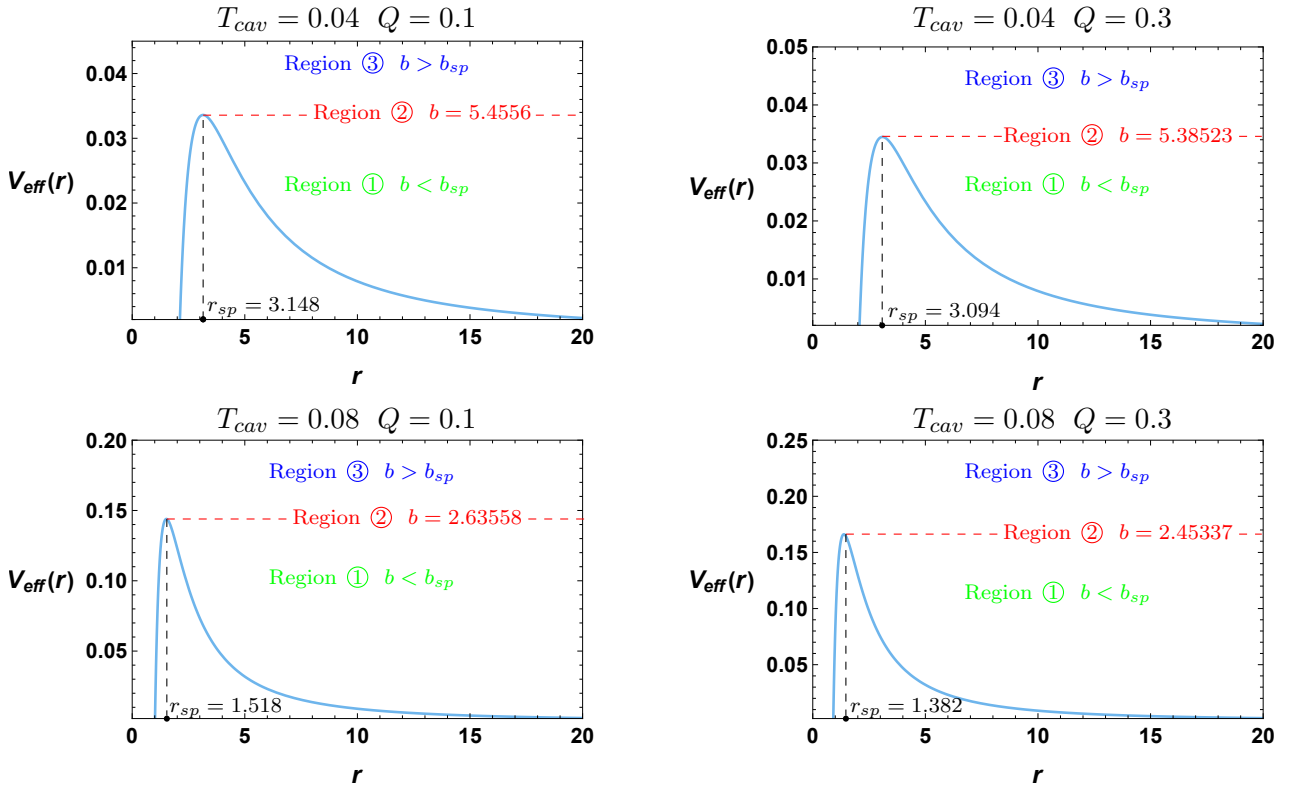


Figure 7: The effective potential behaviors for different values of the charges and the cavity temperature, by taking the cavity radius $r_{cav} = 20$.

This potential increases and reaches a maximum at the photon sphere associated with b_{sp} representing the impact parameter of the spinning light rays. This quantity verifies the following constraint

$$V_{eff}(r_{sp}) = \frac{1}{b_{sp}^2}. \quad (5.2)$$

Two values of T_{cav} will be dealt with, being $T_{cav} = 0.04, 0.08$. For $Q = 0.3$, they provide two impact parameter values $b_{sp} = 5.39$ and $b_{sp} = 2.46$, as shown in Fig.(7), corresponding to

the photon sphere radius $r_{sp} = 3.09$ and $r_{sp} = 1.38$, respectively. For $Q = 0.1$, however, the corresponding impact parameter and the photon sphere radius increase. Fixing the charge values, the effective potential increases by decreasing the cavity temperature. We observe that the photon sphere radius r_{sp} also decreases by increasing the cavity temperature. It has been remarked that the impact parameter value b_{sp} provides the trajectories of the light rays in three different regions. These regions are denoted by region ①, region ② and region ③ corresponding to $b < b_{sp}$, $b = b_{sp}$ and $b > b_{sp}$, respectively.

In the region ①, the light ray falls into the black hole in a cavity due to the values of the impact parameter lower to b_{sp} . In region ③, however, the light rays near the black hole in a cavity system are reflected back. In the region ②, the light ray comes into the photon sphere making an infinite turn number around the black hole due to the non vanishing value of the angular velocity. The associated orbit is circular and unstable. To illustrate these regions, we plot in Fig.(8) the trajectories of the light rays in the polar coordinates (r, ϕ) for different values of the cavity temperature T_{cav} and the charge Q . To analyse the effect of the cavity temperature in the light ray trajectories, we vary the impact parameter b in the range $[0, 7]$. The step between two values of the impact parameter is $1/10$ for all light rays. A close examination reveals that the horizon and the sphere photon radius decrease by increasing the cavity temperature. For fixed values of the charge, this confirms the previous results associated with the shadow and the photon sphere as functions of the cavity temperature. For $T_{cav} = 0.04$, it has been remarked that the region ③ is small than the region ①. An inverse behavior is observed for $T_{cav} = 0.08$. For such a value, the region ③ is large compared to the region ①. Moreover, the region of the reflected light rays enlarges with the cavity temperature. This shows that such a temperature can be considered as a relevant quantity modifying the light ray behaviors near a black hole. However, the charge does not affect such trajectories. An examination shows that the light ray behaviors of the black holes in a cavity system are different than the light trajectories around the non rotating black holes without cavities including the (DE) contributions [9, 21]. It has been observed that such a distinction comes from the cavity effect on the black hole object.

By numerically examining the optical behavior plotted in the above figures, we collect certain optical results for various moduli space regions in Tab.(1).

According to the reported data, we explore certain universal optical ratios. This could be understood as universal optical behaviors completing the ones obtained in the black hole thermodynamics [51, 52]. For small values of the charge Q and the cavity temperature T_{cav} , we observe the following universal optical ratio

$$\frac{b_{sp}}{r_{sp}} \sim \sqrt{3}. \quad (5.3)$$

This universal ratio has not been observed only in the black hole in a cavity but also in the ordinary Schwarzschild (SH) black holes without a cavity. After a consistence verification, we find

$$\frac{b_{sp}(SH)}{r_{sp}(SH)} = \frac{3\sqrt{3}m}{3m} = \sqrt{3}. \quad (5.4)$$

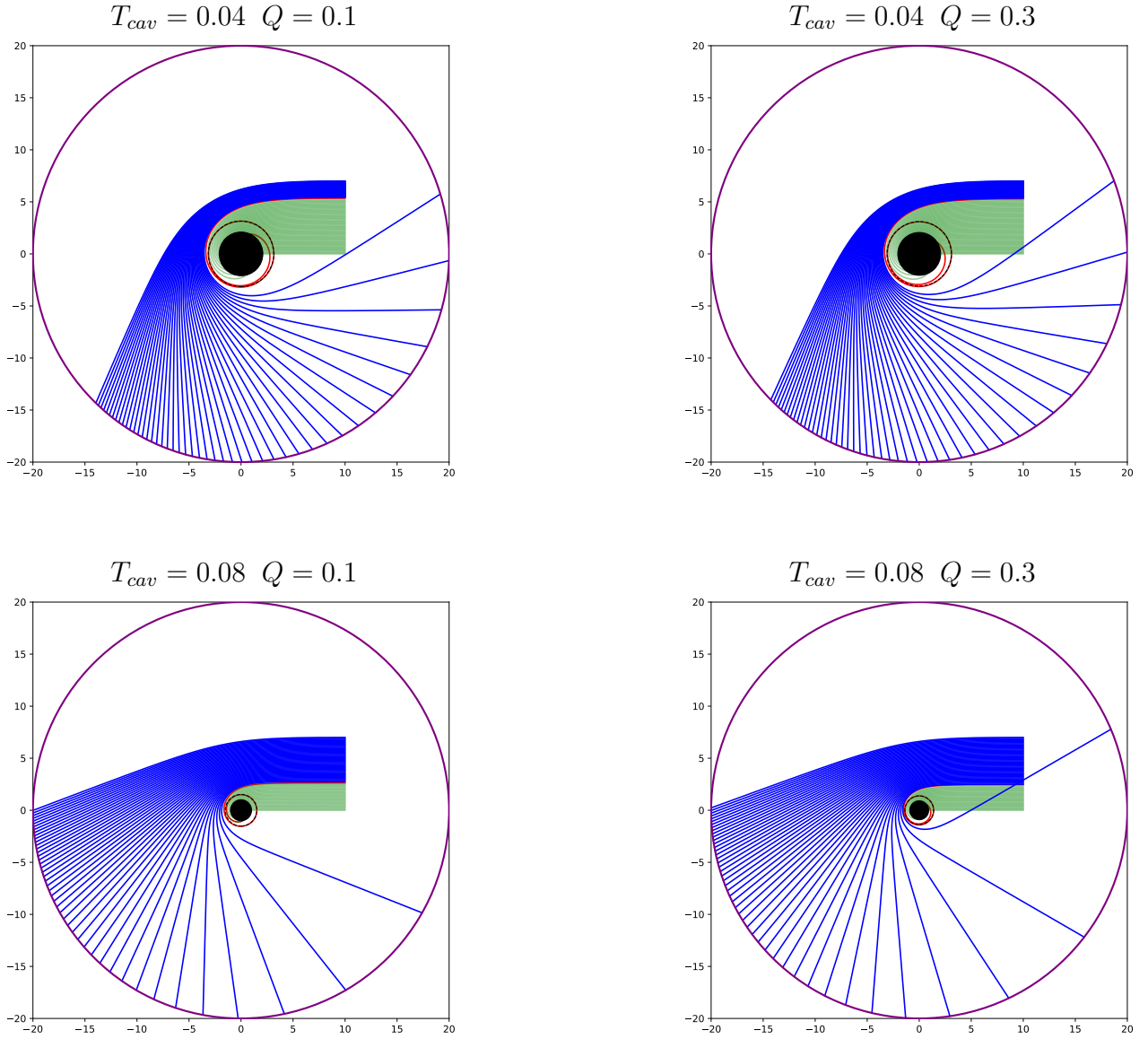


Figure 8: *The trajectories of the light ray for different values of the cavity temperature. The horizon r_+ and sphere photon r_{sp} are represented by the black disc and black dashed circle, respectively. The observer is situated in the equatorial plane and positioned in $r_{ob} = 15$, we take the cavity radius $r_{cav} = 20$.*

In the charged solution, this ratio is checked to be close to $\sqrt{3}$.

6 Conclusion and open questions

In this work, we have explored the optical behaviors of the black holes in a cavity. Concretely, we have studied the shadows and the photon rings of the black holes surrounded by a cavity,

		$T = 0.02$	$T = 0.03$	$T = 0.04$	$T = 0.05$
Q=0.1	b_{sp}	11.75	7.44	5.46	4.31
	r_{sp}	6.78	4.29	3.15	2.49
	$\frac{b_{sp}}{r_{sp}}$	1.73	1.73	1.73	1.73
Q=0.2	b_{sp}	11.73	7.42	5.43	4.27
	r_{sp}	6.77	4.28	3.13	2.46
	$\frac{b_{sp}}{r_{sp}}$	1.73	1.73	1.74	1.74
Q=0.3	b_{sp}	11.71	7.39	5.39	4.22
	r_{sp}	6.76	4.26	3.09	2.42
	$\frac{b_{sp}}{r_{sp}}$	1.73	1.74	1.74	1.75
Q=0.4	b_{sp}	11.69	7.34	5.32	4.12
	r_{sp}	6.73	4.22	3.04	2.34
	$\frac{b_{sp}}{r_{sp}}$	1.74	1.74	1.75	1.76
Q=0.5	b_{sp}	11.65	7.28	5.22	3.97
	r_{sp}	6.71	4.17	2.97	2.23
	$\frac{b_{sp}}{r_{sp}}$	1.74	1.74	1.76	1.78

Table 1: The values of the ratio $\frac{b_{sp}}{r_{sp}}$ for different values of the cavity temperature and the charge Q . The observer in the equatorial plane and positioned in $r_{ob} = 15$, where one has used the cavity radius $r_{cav} = 20$.

where the effect of the temperature and the charge have been examined. After studying the effect of the horizon radius on the observational images of the black holes by varying the charge, we have investigated thermal shadow behaviors in the cavity system with certain geometric conditions. For fixed charge values, we have revealed that the shadow radius r_s increases by decreasing the cavity temperature T_{cav} . Moreover, we have shown that the $r_s - T_{cav}$ curves involve swallowtail behaviors observed in the $G - T$ plane of the ordinary AdS black holes. Among others, we have found that the T_{HP} temperature in the $G - T$ curves coincides with the T_{HP} temperature in the $r_s - T_{cav}$ plane. The present findings could support the relation between the thermodynamics and the optical aspect of the black holes in a cavity.

In this way, certain thermodynamical quantities of the black holes including the phase transition temperature T_{HP} could be approached using the shadow formalism in cavity systems. Then, we have established the trajectory of the light rays casted by the black holes in cavities. Precisely, we have observed that the light trajectories of the black holes in a cavity system are different than the light ray behaviors of the ordinary solutions. This distinction comes from the cavity effect on the black hole object. Finally, we have found an optical universal ratio associated with the photon sphere radius and the impact parameter. For small values of the charge Q and the cavity temperature T_{cav} , we have found the optical ratio $\frac{b_{sp}}{r_{sp}} \sim \sqrt{3}$. This universal optical ratio has been verified for the Schwarzschild black hole without a cavity which equals to $\sqrt{3}$.

This work comes up with certain questions. This study could be adopted to various models by enlarging the moduli space parameter. Rotating black holes in a cavity could be considered as possible extensions even the associated computations will be complicated. It should be interesting also to consider generic optical pictures by approaching different aspects including the deflection angle of the light rays. We hope address such questions in future

works.

Acknowledgments

The authors would like to thank N. Askour, H. El Moumni and Y. Hassouni, for collaborations on related topics. This work is partially supported by the ICTP through AF.

References

- [1] K. Akiyama and al., *First M87 Event Horizon Telescope Results. IV. Imaging the Central Supermassive Black Hole*, *Astrophys. J.* **L4** (1) (2019) 875, [arXiv:1906.11241](#).
- [2] K. Akiyama and al., *First M87 Event Horizon Telescope Results. V. Imaging the Central Supermassive Black Hole*, *Astrophys. J.* **L5** (1) (2019) 875.
- [3] K. Akiyama and al., *First M87 Event Horizon Telescope Results. VI. Imaging the Central Supermassive Black Hole*, *Astrophys. J.* **L6** (1) (2019) 875.
- [4] A. Belhaj, H. Belmahi, M. Benali, H. El Moumni, M. A. Essebani and M. B. Sedra, *Optical shadows of rotating Bardeen-AdS black holes*, *Mod. Phys. Lett. A* **37** (2022) 2250032, [arXiv:2202.10892](#).
- [5] H. Khodabakhshi, A. Giaimo and R. B. Mann, *Einstein Quartic Gravity: Shadows, Signals, and Stability*, *Phys. Rev. D* **102** (2020) 044038, [arXiv:2006.02237](#).
- [6] S. W. Wei, Y. C. Zou, Y. X. Liu and R. B. Mann, *Curvature radius and Kerr black hole shadow*, *JCAP* **08** (2019) 030, [arXiv:1904.07710](#).
- [7] S. Chandrasekhar, *The mathematical theory of black holes*, Oxford University Press, 1998.
- [8] İ. Çimdiker, D. Demir and A. Övgün, *Black hole shadow in symmergent gravity*, *Phys. Dark Univ.* **34** (2021) 100900, [arXiv:2110.11904](#).
- [9] M. Okyay and A. Övgün, *Nonlinear electrodynamics effects on the black hole shadow, deflection angle, quasinormal modes and greybody factors*, *JCAP* **01** (2022) 009, [arXiv:2108.07766](#).
- [10] A. Övgün, I. Sakalli and J. Saavedra, *Shadow cast and Deflection angle of Kerr-Newman-Kasuya spacetime*, *JCAP*. 10 (2018) 041, [arXiv:1807.00388](#).
- [11] A. Grenzebach, V. Perlick and C. Lämmerzahl, *Photon Regions and Shadows of Accelerated Black Holes*, *Int. J. Mod. Phys. D* **24** (2015) 1542024, [arXiv:1503.03036](#).

- [12] A. He, J. Tao, Y. Xue and L. Zhang, *Shadow and Photon Sphere of Black Hole in Clouds of Strings and Quintessence*, Chin. Phys. C **46** (2022) 065102, [arXiv:2109.13807](#).
- [13] A. Grenzebach, V. Perlick and C. Lämmerzahl, *Photon Regions and Shadows of Kerr-Newman-NUT Black Holes with a Cosmological Constant*, Phys. Rev. D **89** (2014) 124004, [arXiv:1403.5234](#).
- [14] H. C. D. L. Junior, P. V. P. Cunha, C. A. R. Herdeiro and L. C. B. Crispino, *Shadows and lensing of black holes immersed in strong magnetic fields*, Phys. Rev. D **104** (2021) 044018, [arXiv:2104.09577](#).
- [15] H. C. D. Lima Junior, L. C. B. Crispino, P. V. P. Cunha and C. A. R. Herdeiro, *Can different black holes cast the same shadow?*, Phys. Rev. D **103** (2021) 084040, [arXiv:2102.07034](#).
- [16] S. Vagnozzi, L. Visinelli, *Hunting for extra dimensions in the shadow of M87**, Phys. Rev. D **100** (2019) 024020, [arXiv:1905.12421](#).
- [17] A. Allahyari, M. Khodadi, S. Vagnozzi, D. F. Mota, *Magnetically charged black holes from non-linear electrodynamics and the Event Horizon Telescope*, JCAP 2002 (2020) 003, [arXiv:1912.08231](#).
- [18] M. Khodadi, A. Allahyari, S. Vagnozzi, D. F. Mota, *Black holes with scalar hair in light of the Event Horizon Telescope*, JCAP 2009 (2020) 026, [arXiv:2005.05992](#).
- [19] C. Bambi, K. Freese, S. Vagnozzi, L. Visinelli, *Testing the rotational nature of the supermassive object M87* from the circularity and size of its first image*, Phys. Rev. D **100** (2019) 044057, [arXiv:1904.12983](#).
- [20] A. Belhaj, M. Benali, H. E. Moumni, M. A. Essebani, M. B. Sedra and Y. Sekhmani, *Thermodynamic and Optical Behaviors of Quintessential Hayward-AdS Black Holes*, Inter. Jour. of Geom. Meth in Mod. Phys, (2022) 2250096, [arXiv:2202.06290](#).
- [21] A. Belhaj, M. Benali, A. El Balali, H. El Moumni and S. E. Ennadifi, *Deflection angle and shadow behaviors of quintessential black holes in arbitrary dimensions*, Class. Quant. Grav. **37** (2020) 215004. [arXiv:2006.01078](#).
- [22] A. Belhaj, H. Belmahi and M. Benali, *Superentropic AdS black hole shadows*, Phys. Lett. B **821** (2021) 136619, [arXiv:2110.06771](#).
- [23] A. Belhaj, H. Belmahi, M. Benali, W. El Hadri, H. El Moumni and E. Torrente-Lujan, *Shadows of 5D black holes from string theory*, Phys. Lett. B **812** (2021) 13602, [arXiv:2008.13478](#).

- [24] A. Belhaj, M. Benali, A. E. Balali, W. E. Hadri and H. El Moumni, *Cosmological constant effect on charged and rotating black hole shadows*, Int. J. Geom. Meth. Mod. Phys. **18** (2021) 2150188. *arXiv:2007.09058*.
- [25] A. Belhaj, M. Benali, A. El Balali, W. El Hadri, H. El Moumni and E. Torrente-Lujan, *Black hole shadows in M-theory scenarios*, Int. J. Mod. Phys. D **30** (2021) 2150026, *arXiv:2008.09908*.
- [26] G. A. Marks, F. Simovic and R. B. Mann, *Phase transitions in 4D Gauss–Bonnet–de Sitter black holes*, Phys. Rev. D **104** (2021) 104056, *arXiv:2107.11352*.
- [27] D. Kubiznak and R. B. Mann, *P-V criticality of charged AdS black holes*, JHEP **07** (2012) 033, *arXiv:1205.0559*.
- [28] N. Altamirano, D. Kubiznak and R. B. Mann, *Reentrant phase transitions in rotating anti-de Sitter black holes*, Phys. Rev. D **88** (2013) 101502, *arXiv:1306.5756*.
- [29] D. Kubiznak and F. Simovic, *Thermodynamics of horizons: de Sitter black holes and reentrant phase transitions*, Class. Quant. Grav. **33** (2016) 245001, *arXiv:1507.08630*.
- [30] A. Belhaj, M. Chabab, H. El Moumni, K. Masmar and M. B. Sedra, *On Thermodynamics of AdS Black Holes in M-Theory*, Eur. Phys. J. C **76** (2016) 73, *arXiv:1509.02196*.
- [31] A. Belhaj, M. Chabab, H. El Moumni, K. Masmar, M. B. Sedra and A. Segui, *On Heat Properties of AdS Black Holes in Higher Dimensions*, JHEP **05** (2015) 149, *arXiv:1503.07308*.
- [32] A. Belhaj, A. El Balali, W. El Hadri, M. A. Essebani, M. B. Sedra and A. Segui, *Kerr-AdS black hole behaviors from dark energy*, Int. J. Mod. Phys. D **29** (2020) 2050069.
- [33] A. Belhaj, A. El Balali, W. El Hadri, H. El Moumni and M. B. Sedra, *Dark energy effects on charged and rotating black holes*, Eur. Phys. J. Plus **134** (2019) 422, *arXiv:1912.08687*.
- [34] M. Zhang and M. Y. Guo, *Can shadows reect phase structures of black holes?* Eur. Phys. J. C. **80** (2020) 790.
- [35] A. Belhaj, L. Chakhchi, H. El. Moumni, J. Khalloufi, K. Masmar, *Thermal image and phase transitions of charged AdS black holes using shadow analysis*, Int. J. Mod. Phys. A. **35** (2020) 2050170.
- [36] X. C. Cai, Y. G. Miao, *Can we know about black hole thermodynamics through shadows?*, *arXiv:2107.08352 [gr-qc]*.
- [37] C. Wang et al, *Ruppeiner geometry of the RN-AdS black hole using shadow formalism*, Nucl. Phys. B **976** (2022) 115698.

- [38] S. Guo, G-R. Li, G-P. Li, *Shadow thermodynamics of AdS black hole in regular space-time*, arXiv:2205.04957.
- [39] A. Belhaj, H. Belmahi, M. Benali, A. Segui, *Thermodynamics of AdS black holes from deflection angle formalism*, Phys. Lett. B **817** (2021) 136313.
- [40] H. W. Braden, J. D. Brown, B. F. Whiting and J. W. York, Jr., *Charged black hole in a grand canonical ensemble*, Phys. Rev. D **42** (1990) 3376.
- [41] P. Wang, H. Wu and H. Yang, *Thermodynamic Geometry of AdS Black Holes and Black Holes in a Cavity*, Eur. Phys. J. C **80** (2020) 216, arXiv:1910.07874.
- [42] H. El Moumni and J. Khalloufi, *Nonlinear-Maxwell-Yukawa de-Sitter black hole thermodynamics in a cavity: I– Canonical ensemble*, Nucl. Phys. B **973** (2021) 115593.
- [43] H. El Moumni and J. Khalloufi, *Nonlinear-Maxwell-Yukawa de-Sitter black hole thermodynamics in a cavity: II - Grand canonical ensemble*, Nucl. Phys. B **977** (2022) 115731.
- [44] F. Simovic and R. B. Mann, *Critical Phenomena of Charged de Sitter Black Holes in Cavities*, Class. Quant. Grav. **36** (2019) 014002, arXiv:1807.11875.
- [45] W. B. Zhao, G. R. Liu and N. Li, *Hawking–Page phase transitions of the black holes in a cavity*, Eur. Phys. J. Plus **136** (2021) 981, arXiv:2012.13921.
- [46] R. André and J. P. S. Lemos, *Thermodynamics of d-dimensional Schwarzschild black holes in the canonical ensemble*, Phys. Rev. D **103** (2021) 064069, arXiv:2101.11010.
- [47] M. Zhang and M. Guo, *Can shadows reflect phase structures of black holes?*, Eur. Phys. J. C **80** (2020) 790, arXiv:1909.07033.
- [48] S. W. Wei and Y. X. Liu, *Observing the shadow of Einstein-Maxwell-Dilaton-Axion black hole*, JCAP **11** (2013) 063, arXiv:1311.4251.
- [49] X. X. Zeng, H. Q. Zhang and H. Zhang, *Shadows and photon spheres with spherical accretions in the four-dimensional Gauss–Bonnet black hole*, Eur. Phys. J. C **80** (2020) 872, arXiv:2004.12074.
- [50] X. X. Zeng and H. Q. Zhang, *Influence of quintessence dark energy on the shadow of black hole*, Eur. Phys. J. C **80** (2020) 1058, arXiv:2007.06333.
- [51] A. Belhaj, M. Chabab, H. El Moumni, M. B. Sedra, *On thermodynamics of AdS black holes in arbitrary dimensions*, Chin. Phys. Lett. **29** (2012) 100401, arXiv:1210.4617.
- [52] A. Belhaj, A. El Balali, W. El Hadri, E. Torrente-Lujan, *On Universal Constants of AdS Black Holes from Hawking-Page Phase Transition*, Phys. Lett. B **811** (2020) 135871, arXiv:2010.07837.